

April 8, 2025

We wish to thank the reviewer for their helpful and constructive comments. The reviewer's comments and questions are addressed below.

## Reviewer 1

The manuscript "Spectral Proper Orthogonal Decomposition of Active Wake Mixing Dynamics in a Stable Atmospheric Boundary Layer" by Yalla et al. analyzes four different AWM strategies using SPOD in a stable ABL, relying on numerical simulation results. Apart from the modal analysis, it also investigates the effect of each strategy on the DEL, making an important contribution to further understand and optimize AWM. However, several issues, including one major concern, require attention before publication:

### Major Comment

1. The right panel of Figure 1 exhibits periodic patterns in the free flow around the wake and streamwise streaks that appear unphysical or at least uncommon. Since the entire study relies on these flow fields, their reliability should be validated. Therefore, the origin of these features needs to be thoroughly investigated, and their potential impact on the results must be assessed. One possible cause could be the grid refinements, whose exact locations should still be clarified in the manuscript. Around the assumed positions of these refinements, small-scale waves can be observed in the flow fields, resembling typical dispersion errors in numerical schemes. To verify the correctness of the flow fields, the authors could compare the current refined cases with a case using a uniform grid throughout the entire domain. However, whether the streamwise streaks are also related to grid refinements remains uncertain and might require further explanation. Flow fields showing a larger area around the turbine and its wake could help clarify this issue.

The spurious oscillations in the flow field that the reviewer noticed were a result of a plotting error in ParaView, and not related to any physical phenomenon or grid refinement issues in the flow. We greatly appreciate the reviewer's attention to detail for noticing this issue. Both the hub-height planes and 3D contour visualizations of the flow have been updated with the corrected fields (see Figure 1 in this document). Additionally, a flow field showing a larger extent of the domain is included here, and overlaid with the regions of refinement for the actuated turbine (Figure 2 in this document). Again, there are no longer nonphysical streaks in the flow field near the refinement boundaries. Information clarifying the refinement regions has been added to the manuscript as well.

The reviewer's larger comment about the effects of transitions between refinement zones resonates well with the authors. In this study, the NREL 2.8MW turbine model has been calibrated for a 1.25m resolution region, and the authors do not have the computational resources to run a uniform-resolution case at this level of refinement. Moreover, the SPOD analysis is primarily focused on large-scale, energy containing structures at low Strouhal numbers, which are expected to be fairly robust to changes in resolution, and the cross-flow planes used for the analysis between 2D and 14D are fully contained in the uniform 2.5m resolution region. The setup used here is also consistent with several other large-eddy simulations performed using the ExaWind suite. Nonetheless, the impact of refinement zones

on resolved turbulence and the requirements for subgrid models warrants a more extensive study, which the authors intend to pursue in future work.

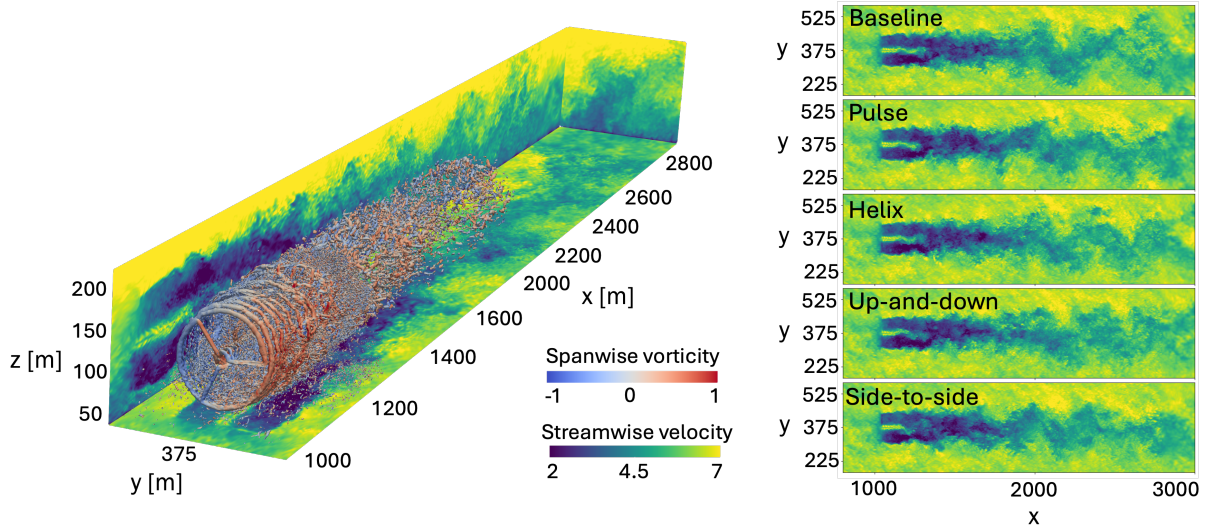


Figure 1: Updated version of Figure 1 in the original manuscript.

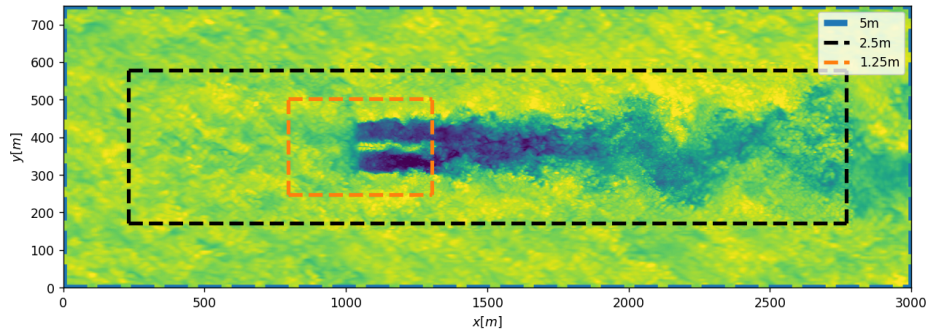


Figure 2: Hub-height visualization of the baseline case, overlaid with the refinement regions around the turbine.

### Further Comments

2. Amplitude Comparison (Lines 142–143 and Figure 5) The "up-and-down" and "side-to-side" cases use double the pitch amplitude compared to the other cases, raising concerns about the fairness of the comparison. This is also critical for the practical implementation of AWM, as the pitch amplitude directly affects the feasibility of applying AWM strategies to real turbines. A stronger initial perturbation likely results in more pronounced wake dynamics while also influencing turbine loads. This discrepancy appears to favor the "up-and-down" and "side-to-side" cases over the helix and pulse strategies. For instance, Figure 12 suggests that the wake differences are more pronounced in these cases. Surprisingly, the "up-and-down" and "side-to-side" cases do not exhibit significantly higher turbine loads, despite the stronger excitation. To ensure a consistent comparison, all cases it would be preferred to maintain the same pitch amplitude, particularly

when evaluating turbine performance and structural loads. The authors should further justify their choice of pitch amplitude and, if necessary, provide additional cases with uniform amplitudes for comparison.

The primary motivation for using double the total pitch amplitude in the up-and-down and side-to-side cases is to ensure that each mode in the SPOD analysis is forced with the same amplitudes by the blade-pitch actuations. This allows for a consistent comparison in terms of modal energy and turbulence entrainment between modes and between AWM cases. Since the SPOD results are the main focus of the paper, the authors feel this is the appropriate setup for the study.

However, from a practical standpoint, the reviewer brings up a good point about the fairness of the comparison. To address this, consider the total pitch travel between cases shown in the following figure:

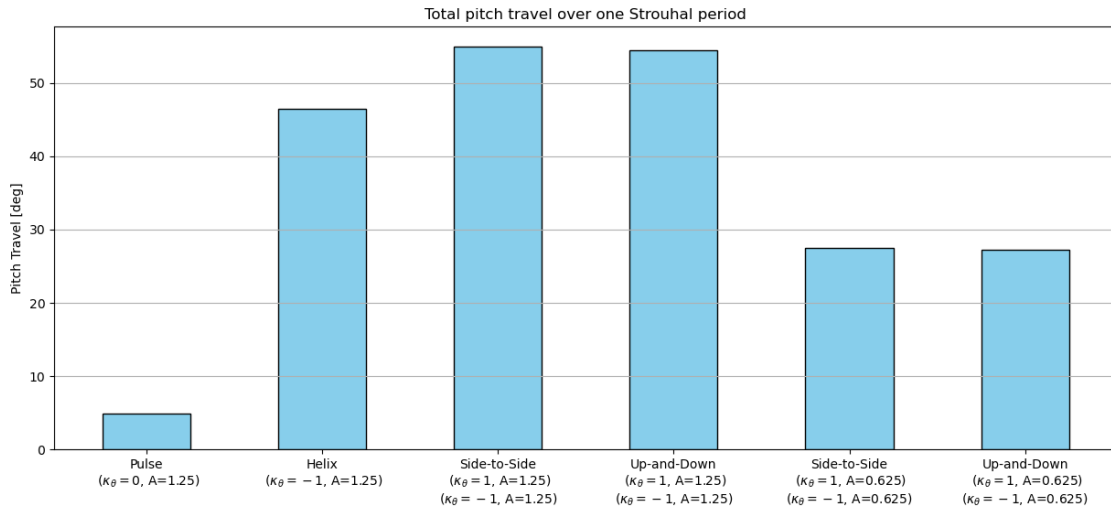


Figure 3: Total pitch travel over one Strouhal period for a single turbine blade

Shown in Figure 3 are the pulse and helix cases at  $A = 1.25^\circ$ , the side-to-side and up-and-down cases with each mode forced at  $A = 1.25^\circ$  ( $2.5^\circ$  total), and the side-to-side and up-and-down cases with each mode forced at  $A = 0.625^\circ$  ( $1.25^\circ$  total). The side-to-side and up-and-down cases with  $2.5^\circ$  total pitch amplitude exhibit an 18% increase in pitch travel over the helix case with  $1.25^\circ$  total pitching amplitude. However, the side-to-side and up-and-down cases with  $1.25^\circ$  total pitching amplitude exhibit over a 40% decrease in pitch travel compared to the helix case. Therefore, the authors feel that setting the pitch amplitude for each mode to  $1.25^\circ$  for all AWM cases provides the most consistent comparison in terms of both modal energy and total pitch travel. Information regarding the total pitch travel has been added to the manuscript (see Figure 4 below), and the motivation for the setup of each AWM case has been clarified.

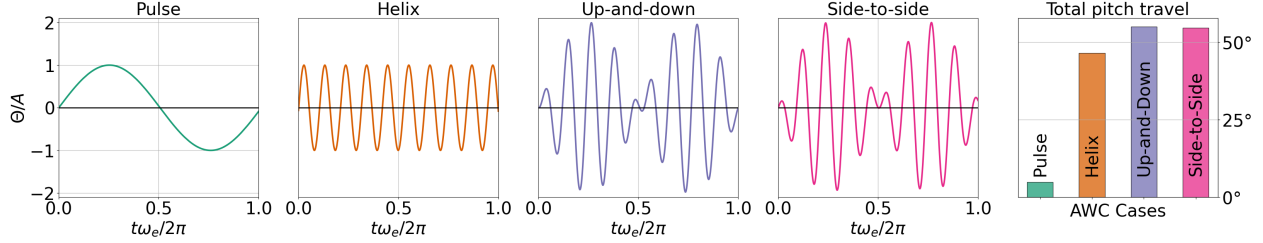


Figure 4: Time series of the blade pitch signal for a single blade for each AWM cases, normalized by the pitching amplitude. One Strouhal period is shown based on the excitation frequency  $\omega_e$ . The black line at  $\Theta/A = 0$  corresponds to the baseline blade pitch signal. The total pitch travel for a single Strouhal period is also shown

3. Several quantities are computed using a rotor disk centered around the wake center instead of the turbine center. Since the wake center also displaces in the vertical direction—something a downstream turbine cannot follow—a turbine-centered approach may provide more applicable insights. This would also help relate the results from Section 3.2 to those in Section 3.3. Would the conclusions change if the rotor disk were centered around the turbine?

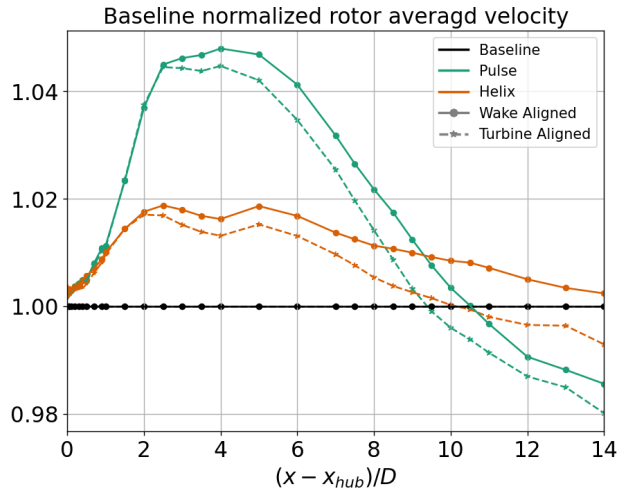


Figure 5: Baseline normalized rotor-averaged velocity for a rotor-disk aligned with the wake center and a rotor-disk aligned with the turbine. In each case, the rotor-disk is aligned vertically with the turbine hub-height. The results for the pulse and helix mixing strategies are shown.

This is a good question from the reviewer concerning where the wake analysis in Sections 3.1 and 3.2 should be centered on, and where the downstream turbine in Section 3.3 should be placed. To be clear, all the results in the manuscript are aligned laterally with the wake, rather than the upstream turbine. This includes the positioning of the downstream turbine in the two-turbine array study presented in Section 3.3. Specifically, as the second turbine is moved in the streamwise direction, its lateral placement is adjusted to follow the center of the wake. This is consistent with the SPOD and entrainment analysis discussed in the preceding sections. The decision to align the results with the wake was made because wake control methods are most useful in fully-waked environments. For example, consider the

baseline-normalized rotor-averaged velocity for a rotor-disk aligned with the upstream turbine compared to a rotor-disk aligned with the lateral-wake center for the pulse and helix strategies (see Figure 5 in this document). At all downstream locations, there is a greater improvement over the baseline for the wake-aligned rotor-averaged velocity than the turbine-aligned rotor-averaged velocity. Note that each rotor disk is aligned vertically with the hub-height in this example. The authors have clarified that the turbine-aligned configuration is not the fully-wake environment in this flow, particularly due to high degree of veer, and that the lateral position of the second turbine in Section 3.3 is changed with downstream position.

Furthermore, we would like to note for the reviewer that the primary trends observed in the baseline-normalized eigenvalues from the SPOD analysis remain largely unchanged when aligned with the turbine’s hub location, rather than the wake center (see Figure 6 in this document). This is particularly true in the near-wake region where the wake has not significantly displaced from the turbine. While we believe that Figure 6 does not need to be included in the manuscript, we have provided it here for the reviewer’s reference to highlight that the results are somewhat robust to this choice.

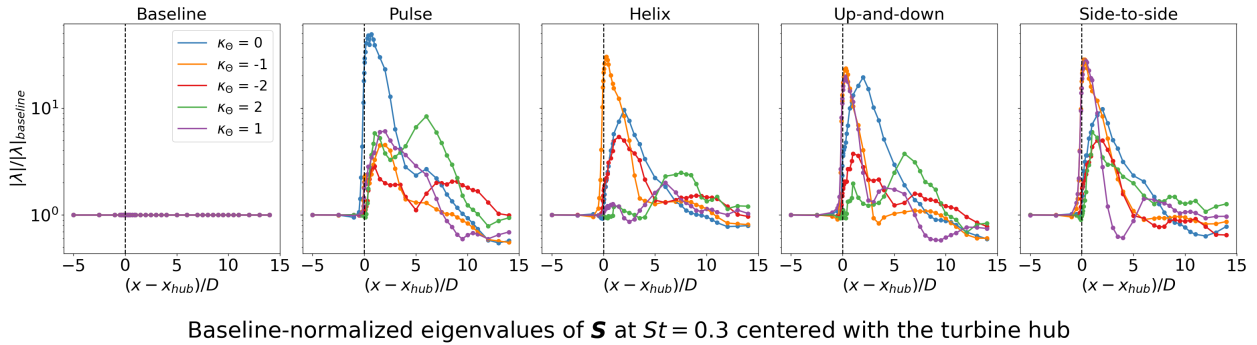


Figure 6: Baseline-normalized SPOD eigenvalues centered on the turbine hub location instead of the wake center.

Lastly, the reviewer is correct that there is a difference in the vertical location that the analysis in Section 3.1 and 3.2 is centered around, and in the placement of the second turbine in Section 3.3, which cannot follow the wake’s vertical movements. The authors acknowledge this difference, but feel it is still appropriate to center the wake analysis with the wake’s vertical and lateral centers to track the primary flow structures throughout their streamwise evolution, since the SPOD analysis is the primary focus of the manuscript. Notably, the vertical displacement of the wake is much smaller than it’s lateral movement, and the performance of the OpenFAST turbine is comparable to the rotor averaged velocity around the wake center. To help strengthen the connection between Sections 3.2 and 3.3, the authors have included the results for the downstream turbines power in the Section 3.3, not just the combined power of the two-turbine array (see Figure 7 in this document). The trends follow very closely with the rotor-averaged velocity reported in Section 3.2.

4. The chosen SPOD parameters resolve Strouhal numbers up to  $St = 0.15$ . Could the observed noise in the higher eigenvalues in Figure 20 be related to unresolved frequencies beyond this range? A sensitivity analysis on the SPOD parameters, such as the length of the time series and their

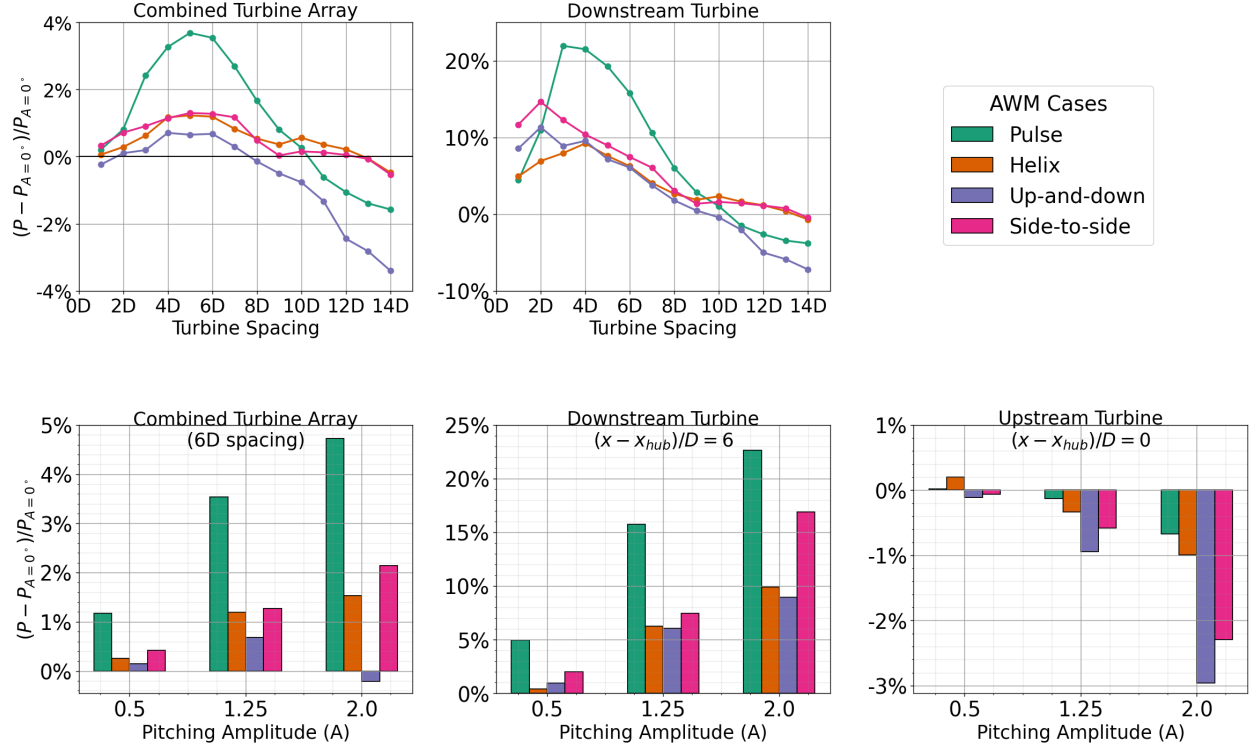


Figure 7: (top) Percent change in generated power,  $P$ , from the baseline case ( $A = 0^\circ$ ) for a two turbine array with the turbine spacings ranging from  $1D$  to  $14D$ . AWM is applied to the upstream turbine with  $A = 1.25^\circ$ , while the downstream turbine is operated using baseline controls. (bottom) Percent change in generated power from the baseline case for the two turbine array with  $6D$  spacing for three different pitching amplitudes applied to the upstream turbine,  $A = 0.5^\circ$ ,  $A = 1.25^\circ$ , and  $A = 2.0^\circ$ . Results for the combined two turbine array, the upstream turbine, and the downstream turbine are shown.

overlap, would help determine whether adjustments can mitigate noise and furthermore strengthen the paper’s overall contribution.

The authors would like to clarify that the oscillations in Figure 20 of the original manuscript are not a result of noise or lack of convergence, but rather the ordering of modal-indices based on  $\tau_{j,j}$  versus  $|\lambda_j|$ . Consider Figure 8 in this document, which shows the spectra of these two quantities  $3D$  downstream, ordered in two different ways. In the top row of Figure 8, the modes are ordered based on their energy content, represented by the corresponding eigenvalue  $|\lambda_j|$ . In the bottom row of Figure 8, the modes are ordered based on their contribution to entrainment, represented by the quantity  $\tau_{j,j}$ . In each case, it may appear as if there is noise in the spectra for the quantity that the indices are not ordered by, i.e.,  $\tau_{j,j}$  in the top row and  $|\lambda_j|$  in the bottom row. However, this is because the SPOD formulation only guarantees a monotonic ordering of modes based on eigenvalues, and there is no reason to expect  $\tau_{j,j}$  to line up with this ordering, especially for smaller turbulent scales. Moreover,  $\tau_{j,j}$  is not necessarily a positive quantity like  $|\lambda_j|$ , so rapid roll-offs in the spectra occur on a log-scale for any modes that lead to a net turbulent entrainment of mean velocity out of the wake. Throughout the manuscript, the modal index,  $j$ , is consistently ordered based on the SPOD

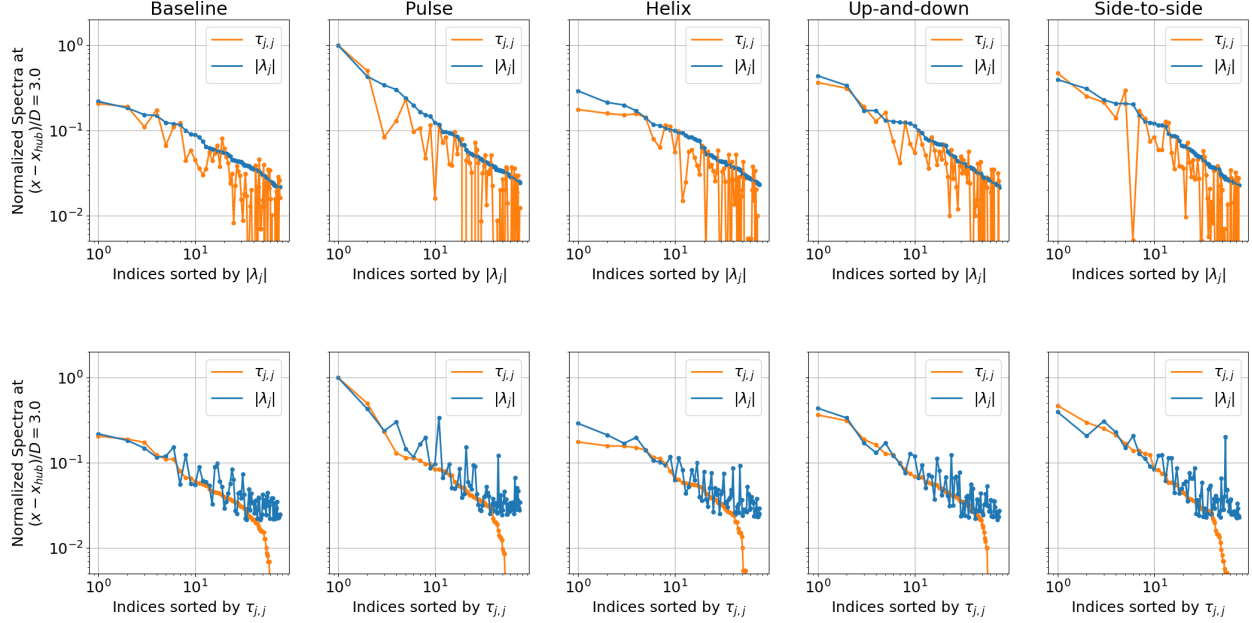


Figure 8: Energy and entrainment spectra defined by  $|\lambda_j|$  and  $\tau_{j,j}$ , respectively, for the leading 75 eigenvalues at  $(x - x_{hub})/D = 3$ .

eigenvalue, as is most natural, and  $\tau_{j,j}$  is plotted with respect to this ordering.

Additionally the authors would like to clarify that Strouhal numbers up to 19.7 are resolved in this study, which should be more than sufficient for representing the larger indices  $j$  that generally correspond to smaller spatio-temporal structures. Moreover, the eigenvalues associated with these scales convergence much more rapidly than the small indices  $j$ , so that convergence is generally not an issue in this region of the spectra. The SPOD parameters in this study were chosen to maximize the number of “blocks” over the 1,100s time interval while ensuring good temporal resolution of the forcing Strouhal number, 0.3, and this justification has been added to the manuscript.

5. Figure 23: Power Improvements at  $A = 0.5$  Degrees The reported power improvements at the actuated turbine at  $A = 0.5$  degrees require further verification. The authors suggest that this might be a regime where the wake does not yet respond to the actuation, yet the downstream turbine loses power, which indicates that the wake reacts, but in an unexpected and unwanted way. Additional analysis, such as energy entrainment or rotor-averaged velocity through the wake, might help clarify this behavior. If verification is not possible, the authors should consider removing the  $A = 0.5$  degree case from the manuscript.

Upon further investigation, an error was identified in the computation of the statistics for the two-turbine array, which resulted in an artificial increase in the power of the upstream turbine at  $A = 0.5^\circ$ . The error involved time-series data being averaged over different intervals between each AWM case and the baseline case, leading to inconsistent comparisons. In the updated results (Figure 7 in this document), the averaging interval has been fixed so that all cases, including the baseline, are averaged over an even number of Strouhal periods. As a result, there is no longer a significant increase in the power of the upstream turbine at

$A = 0.5^\circ$ . Moreover, the power of the downstream turbine now increases with pitching amplitude for all forcing strategies, as is expected. The authors greatly appreciate the reviewer’s suggestion to re-examine these results, leading to these important clarifications.

6. The DEL study does not examine the effects on pitch bearings, which have been identified as a limiting factor in AWM application. Including this additional load channel would enhance the paper’s contribution.

The authors have added a pitch travel metric to the comparisons between AWM cases (see Figure 4 in this document), and kept the DEL study limited to the load channels reported from OpenFAST. The authors acknowledge that pitch travel is not equivalent to pitch-bearing usage, but feel it serves as a sufficient metric for quantifying the difference in pitch-wear between the AWM cases for the purposes of this manuscript.

7. Section 3.3 presents the effect of AWM on the DEL. However, the manuscript does not describe how the DEL is computed. Please add this information to the Methodology or the Appendix, or at least include a reference.

The following two references have been added to the manuscript that the authors followed to compute Damage Equivalent Loads

- Freebury, Gregg, and Walter Musial. “Determining equivalent damage loading for full-scale wind turbine blade fatigue tests.” 2000 ASME wind energy symposium. 2000.
- Ennis, Brandon L., Jonathan R. White, and Joshua A. Paquette. “Wind turbine blade load characterization under yaw offset at the SWiFT facility.” Journal of physics: Conference series. Vol. 1037. No. 5. IOP Publishing, 2018.

8. Consider restructuring the order of the Figures to align more logically with the text’s progression.

The authors have restructured Figures 9 and 10 in the original manuscript to align with the reviewer’s suggestion. The baseline-normalized eigenvalues are now shown together in one figure, with the top row corresponding to the near-turbine region,  $-1 \leq (x - x_{hub})/D \leq 1$ , and the bottom row corresponding to the entire streamwise domain,  $-5 \leq (x - x_{hub})/D \leq 14$  (see Figure ?? in this document). Likewise, the globally-normalized eigenvalues are also shown together in one figure using the same layout (see Figure ?? in this document). We feel this better aligns the figures with the order the analysis. Moreover, Figure 2 in the original manuscript has been removed altogether, in response to the reviewer’s later suggestion. The authors will do their best to position the figures as close to the locations where they are discussed in the paper, and will work with the journal’s editorial team to correct the typesetting and placement of the figures in the final version of the manuscript.

### Minor Issues and Clarity Improvements

The authors have done their best to address all minor issues raised by the reviewer. These suggestions were helpful in improving the clarity of the manuscript. Further responses to a selection of the reviewer comments are included below.

- Line 207: Planes are sampled at a 1.25m resolution, while the grid resolution is at least in parts coarser (2.5m or more). Is it correct that the planes are sampled at a higher resolution than the grid, and if yes, why?

This has been corrected, thank you. The planes are sampled at a spatial resolution consistent with the local grid resolution.

- Figure 6: What causes the fluctuations in modal blade loads around  $x = 0.6 r/R$ , which are absent in the baseline but appear in all AWM cases?

This behavior has been previously observed for the NREL 2.8MW turbine model, even for canonical flow conditions [Cheung et al., 2024], and is currently under further investigation. The authors suspect that these fluctuations may be an artifact of the blade model rather than a result of the computation of the axial force spectra. The authors are interested to see if these fluctuations arise for other turbine models as well.

- Figure 24: The upper limit of the y-axis is significantly higher than the highest bar, creating excessive white space and making it difficult to distinguish between the bars for the upstream and downstream turbines. Adjust the upper limit for clearer presentation of the results.

Figure 24 of the original manuscript has been revised so that the y-axes are no longer unified across load channels (see Figure 9 in this document). Please note that some of the additional white space in the figures arises from the values of the DLC 1.2 case, which provides important context for the baseline loads.

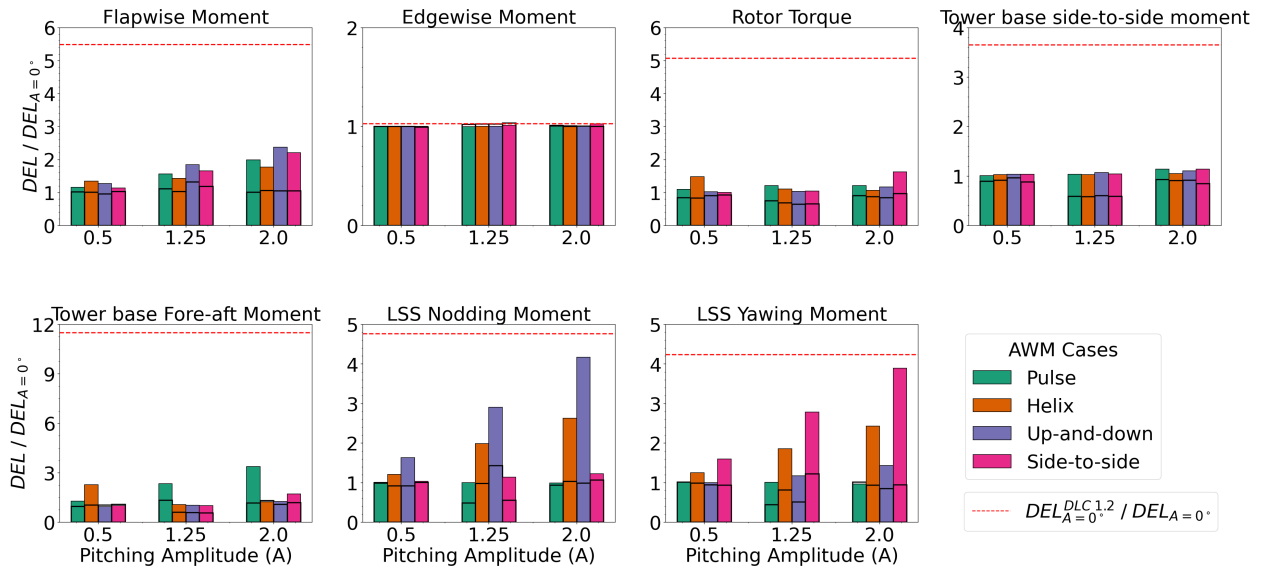


Figure 9: Baseline-normalized damage equivalent loads (DEL) for seven different load channels at three different pitching amplitudes,  $A = 0.5^\circ$ ,  $A = 1.25^\circ$ , and  $A = 2.0^\circ$ . Solid bars indicate DELs for the upstream turbine, while the DELs for the turbine  $6D$  downstream are outlined in black. The red dashed line corresponds to the baseline-normalized DELs from a normal turbulence model in a DLC 1.2-like environment (single seed) with a hub height wind speed of 6.4 m/s, a shear exponent of 0.12, and a turbulence intensity of 25.90%.

- Consider citing the work by Muscari et al. "Physics-Informed DMD for Periodic Dynamic Induction Control of Wind Farms" (DOI: 10.1088/1742-6596/2265/2/022057) in the Introduction. Citation: <https://doi.org/10.5194/wes-2025-14-RC1>.

Thank you for the relevant reference — a citation has been added to the manuscript.

## References

Lawrence C Cheung, Kenneth A Brown, Daniel R Houck, and Nathaniel B deVelder. Fluid-dynamic mechanisms underlying wind turbine wake control with strouhal-timed actuation. Energies, 17 (4):865, 2024.